

# Evaporation of superfluid helium in a capillary

C.R. Lages\*, R.H. Torii and D.B. DeBra\*

W.W. Hansen Experimental Physics Laboratory, Stanford University, Stanford, CA 94305-4085, USA

\*Department of Aeronautics and Astronautics, Stanford University, Stanford, CA 94305, USA

Received 26 May 1994; revised 9 August 1994

The steady-state evaporation of superfluid helium at a liquid–vapour interface near the exit of a cylindrical capillary is considered. In order to maintain phase equilibrium, as the evaporation rate increases the liquid–vapour interface will retreat into the capillary. Due to the very large density difference between the liquid and vapour, the retreat of the interface into the capillary produces a sharp change in mass flow. A simple capillary model has been applied to flow in porous plug phase separators by considering parallel capillaries of equal length but with a distribution of diameters. In this case it is found that the change in mass flow is consistent with what has been observed for an increasing pressure drop across a porous plug. This suggests that the equilibrium flow states occur as the liquid–vapour interface retreats into a porous plug in response to incremental increases in the pressure drop across the plug.

**Keywords:** porous plug phase separators; superfluid helium; evaporation

Recent low temperature experiments in space have shown that long term thermal stability can be achieved through controlled evaporation of superfluid helium at the surface of a porous metal sponge (porous plug phase separator)<sup>1–3</sup>. The function of the porous element is two-fold: (1) capillary forces ensure a supply of liquid; and (2) the thermomechanical effect in superfluid helium allows for thermal regulation of the mass flow. Future high-precision experiments in space, for example, the Relativity Mission and STEP, require not only thermal stability, but a sufficient mass flow to provide the thrust needed to compensate for disturbance forces due to air drag. This added requirement on the mass flow may lead to the use of the porous element in a mass flow region which is not well understood.

Previous experiments<sup>4–6</sup> on porous plug phase separators have shown that the mass flow can be divided into at least two flow regimes (see *Figure 1b*). These two regions are separated by a sharp slope change in the plot of mass throughput *versus* pressure drop across the plug. The region of small mass flow is believed to be linear and can be correlated to the pore geometry via a constant impedance factor which can be determined by a separate measurement (e.g. vapour flow at room temperature). The region beyond the slope change as well as the dynamic behaviour of the transition between the two regions are not well understood. In fact, a number of experiments have shown that mass flow in the region is hysteretic, i.e. an increasing pressure drop produces a different mass flow than a decreasing pressure drop (see the inset of *Figure 1b*)<sup>4–6</sup>. Such non-linear behav-

our can obviously lead to unacceptable performance of spacecraft control systems which rely on the porous plug.

Starting from an earlier paper which argued that the origin of the mass flow change is due to the liquid–vapour phase boundary retreating into the plug<sup>4</sup>, we model the porous plug by considering a straight cylindrical capillary. We then ask the question under what mass flow conditions is it possible to have the coexistence of liquid and vapour in the capillary? Rather than pursue arguments based on a balance of mechanical forces at the liquid–vapour interface<sup>4</sup>, we base our analysis on conditions of mass flow continuity and phase equilibrium. A similar approach has been used in petroleum engineering studies of classical two-phase flow in porous media<sup>7</sup>. In the case of superfluid helium, however, the situation is slightly more complicated.

As is well known, the laminar flow of superfluid helium can be described by the two-fluid model. For evaporation from a cylindrical capillary of diameter  $d$ , this leads to a net mass flow per unit area  $\dot{m}$ , given by<sup>8</sup>

$$\dot{m} = \frac{d^2(\rho S)^2 T}{32\eta(\lambda + ST)} \left| \frac{dT}{dx} \right| \quad (1)$$

where:  $\rho$  is liquid density;  $S$  is liquid entropy;  $T$  is the temperature in the liquid;  $\eta$  is the normal fluid viscosity;  $\lambda$  is the latent heat of vaporization; and  $x$  is the distance along the capillary. We have ignored the thermal conductivity of the capillary and consider only heat conduction by the fluid. The temperature gradient along the capillary is taken to be

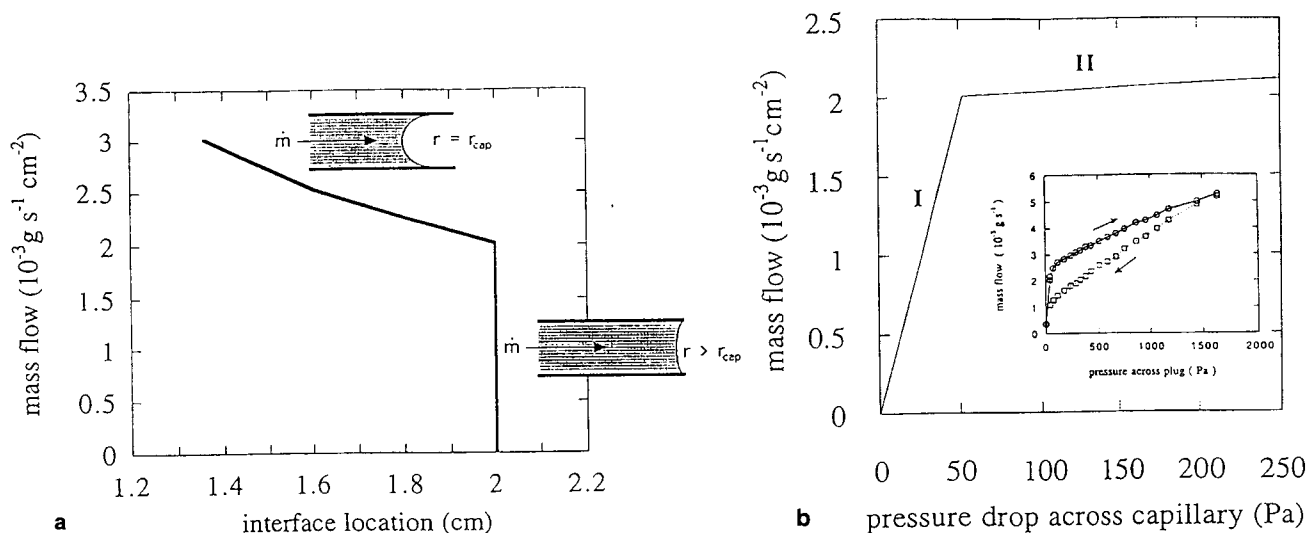


**Figure 1** (a) Equilibrium position of liquid–vapour interface for a given mass flow through a capillary of 2  $\mu\text{m}$  diameter and 2 cm length. (b) Mass flow versus pressure drop across the capillary. The inset is a plot of the experimental data of Murakami *et al.*<sup>5</sup>

small ( $dT/dx \ll T$ ) and can be related to the pressure gradient along the capillary by

$$\frac{dP_L}{dx} = \rho S \frac{dT}{dx} \quad (2)$$

where  $P_L$  is the liquid pressure. Thus, using (1) and (2), for a given evaporation rate  $\dot{m}$  we can find the temperature and pressure in the liquid along the capillary. For the vapour, we consider laminar flow.

In order to determine the location of phase transition, we use a thermodynamic analysis and assume that at the liquid–vapour interface the evaporation takes place reversibly at a constant temperature  $T$ . The location of the liquid–vapour interface along the capillary is determined by the condition

$$\mu_L(T, P_L) = \mu_V(T, P_V) \quad (3)$$

where  $\mu_L$ ,  $P_L$  are the chemical potential and pressure of the liquid and  $\mu_V$ ,  $P_V$  are the chemical potential and pressure of the vapour. For a flat liquid–vapour interface,  $P_L = P_V \equiv P_o$ . In the capillary, however, the interface is no longer flat but curved. Given that the liquid wets the wall (contact angle is zero), let us take for the interface in the capillary a surface with a radius of curvature  $d/2$ , where  $d$  is the diameter of the capillary. The liquid and vapour pressures  $P_L$  and  $P_V$  are no longer equal but given by

$$P_V - P_L = \frac{4\sigma_{LV}}{d} \quad (4)$$

where  $\sigma_{LV}$  is the liquid–vapour surface energy. It is important to note that on a curved interface the liquid and vapour no longer coexist on the saturation line,  $P_o(T)$ , as defined by the thermodynamic equilibrium of a flat liquid–vapour interface. In fact, deviation from  $P_o(T)$  can be significant. It is straightforward to show that both the liquid and vapour pressures are lowered from their nominal equilibrium value regardless of pressurization of the liquid, and result in a phase transition between a superheated liquid and a superheated vapour. The liquid pressure is lowered by a significant amount for pore diameters less than 100  $\mu\text{m}$ ,

whereas vapour pressure lowering can be neglected for pore diameters larger than 0.1  $\mu\text{m}$ .

It becomes clear then that in order to find a phase boundary along the capillary which satisfies the conditions of phase equilibrium we must also know the thermodynamic properties of the superheated liquid. For the free energy of the superheated liquid, we use a linear extrapolation of the tabulated bulk free energy data. The vapour free energy can also be found through extrapolation by assuming the vapour to be an ideal gas. We can now find the position of the liquid–vapour interface in the following way. For a given mass flow  $\dot{m}$ , we calculate the pressure and temperature distribution for either liquid or vapour flow in the capillary. From the temperature and pressure distributions, we can calculate the chemical potential for the liquid and the vapour along the capillary. For a given equilibrium position in the capillary, as defined by (3) and (4), we then check the vapour flow and make sure that the temperature and pressure at the exit of the capillary are correct.

*Figure 1a* shows the result of our calculations for the position of the liquid–vapour interface in the capillary. As the mass flow is increased, the radius of curvature of the liquid–vapour interface at the capillary exit decreases until it becomes equal to the radius of the capillary. Further increases in the mass flow lead to retreat of the phase boundary into the capillary. In *Figure 1b*, we plot our results for a capillary of 2  $\mu\text{m}$  diameter and 2 cm length as mass flow versus pressure drop across the capillary. The two different flow regimes can be clearly seen and are labelled I and II. Also plotted in the inset of *Figure 1b* are the experimental data of Murakami *et al.*<sup>5</sup>. The results of our calculation are qualitatively consistent with what has been seen by experiment. There are, however, two obvious flaws with this simple model. The first is a geometry problem, in that porous media are not defined by a single pore diameter but rather by a distribution of pore diameters. In addition, there is also a tortuosity associated with porous media due to the fact that the pores are far from straight. The second problem is that our single capillary model cannot explain the hysteresis observed in region II (see the inset of *Figure 1b*).

In an attempt to address the first of these problems, we have considered the evaporation from parallel capillaries of

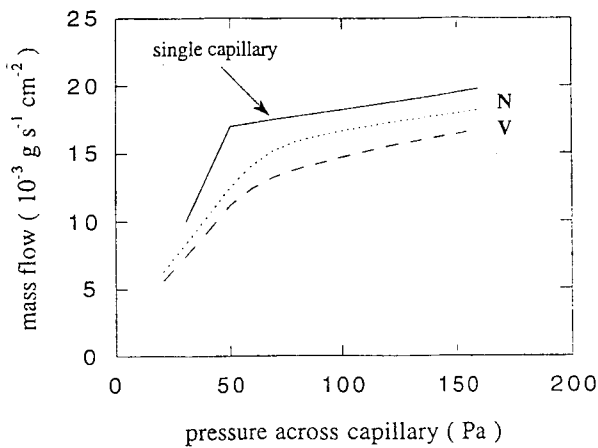


**Figure 2** Comparison of mass flow versus pressure drop for a single capillary to that of a distribution of capillaries. For the two distributions shown, the pore radii range from 0.5 to 8  $\mu\text{m}$ . The curve labelled N is for a uniform distribution of pore number and the curve labelled V is for a uniform distribution of pore volume. The single capillary curve as well as the uniform pore volume distribution curve have been scaled for the purposes of comparison

equal length but of different pore diameters. The capillaries are taken to have the same temperature and pressure at each entrance and exit but are otherwise independent. The results for two different pore diameter distributions along with the result for a single capillary are shown in *Figure 2*. For both distributions, the pore diameters range from 1 to 16  $\mu\text{m}$ . The difference between the two distributions is that for the curve labelled N we take a uniform distribution of pore number and in the curve labelled V we take a uniform distribution of pore volume. We see from *Figure 2* that the effect of a distribution of pore diameters is to smooth the transition from region I to II. The significant point to note is that the shape of the curve is similar to the transition which has been seen for an increasing pressure drop across the porous plug (see the inset of *Figure 1b*)<sup>4-6</sup>.

Thus, it is the change in mass flow seen for a decreasing pressure drop across the porous plug (see the inset of *Figure 1b*) which is very peculiar and perhaps cannot be explained by our model. For this reason, we are currently working on a network model to see what type of flow transition is produced by a network of capillaries (which have varying lengths and diameters) in the process of filling with a superfluid.

## Conclusions

In summary, we have shown that the thermodynamics of evaporation from a cylindrical capillary supports the idea of phase boundary retreat. We have also demonstrated that for a distribution of pore diameters the transition from region I to II compares better with the transition seen for an incrementally increasing pressure drop across a porous plug. This says that the upper flow branch of the hysteresis loop is the equilibrium state. The transition for a decreasing pressure drop needs further study and perhaps a more complicated model. In particular, we believe a network model may solve this problem. This will help us to understand the true limits of porous plug devices (phase separators and thermomechanical pumps) for use in future spacecraft relying on high-precision thermal and cryogenic propulsion systems.

## Acknowledgements

We would like to thank S.W.K Yuan and J.C. Mester, Jr for useful discussions and for reading the manuscript. This work was supported by NASA through contract NAS8-36125 (Gravity Probe B Experiment) and JPL contract 959723 (QuickSTEP Experiment). CRL was also supported by a fellowship from Rockwell International and performed the work in partial fulfillment of a PhD in the Department of Aeronautics and Astronautics at Stanford University.

## References

- 1 Urbach, A.R. and Mason, P.V. IRAS cryogenic system flight performance report *Adv Cryog Eng* (1984) **29** 651
- 2 Mason, P.V., Petrac, D., Elleman, D.D., Wang T. *et al.* Preliminary results of the Spacelab 2 superfluid helium experiment *Adv Cryog Eng* (1986) **31** 869-879
- 3 Volz, S.M., DiPirro, M.J., Castles, S.H., Ryschkewitsch, M.G. *et al.* Final cryogenic performance report for the NASA Cosmic Background Explorer (COBE) *Adv Cryog Eng* (1992) **37** 1183-1192
- 4 DiPirro, M.J. and Zahniser, J. The liquid/vapour phase boundary in a porous plug *Adv Cryog Eng* (1990) **35** 173-180
- 5 Murakami, M. and Nakai, H. Flow phenomena of superfluid helium through a porous plug phase separator *Cryogenics* (1987) **27** 442-449
- 6 Elliott, D.G. Porous plug tests and flow modeling for the Space Infrared Telescope Facility (SIRTF). JPL Publication JPL D-11412 (June 1994)
- 7 Udell, K.S. Heat transfer in porous media heated from above with evaporation, condensation, and capillary effects *ASME J Heat Transfer* (1983) **105** 485-492
- 8 Schotte, U. He II phase separation with slits and porous plugs for space cryogenics *Cryogenics* (1984) **24** 536-547